2014

Modeling And Predictive Control Of High Performance Buildings With Distributed Energy Generation And Thermal Storage

Siwei Li
Purdue University, School of Civil Engineering, West Lafayette, Indiana, USA., li613@purdue.edu

Panagiota Karava
Purdue University, School of Civil Engineering and Division of Construction Engineering and Management, West Lafayette, Indiana, USA., pkarava@purdue.edu

Follow this and additional works at: http://docs.lib.purdue.edu/ihpbc

Modeling and Predictive Control of High Performance Buildings with Distributed Energy Generation and Thermal Storage

Siwei LI[1], Panagiota KARAVA[2*]

[1]Purdue University, School of Civil Engineering,
West Lafayette, Indiana, USA
Contact information (+1-765-494-1714, li613@purdue.edu)

[2]Purdue University, School of Civil Engineering and Division of Construction Engineering and Management,
West Lafayette, Indiana, USA
Contact information (+1-765-494-4573, +1-765-494-0644, pkarava@purdue.edu)

* Corresponding Author

ABSTRACT

The paper explores integration approaches of photovoltaic-thermal systems coupled with corrugated transpired solar collectors (building-integrated photovoltaic-thermal, BIPV/T), Heating, Ventilation and Air Conditioning (HVAC) systems and thermal storage devices, to enable optimal collection and utilization of solar energy in high performance buildings. An open plan office space at Purdue's Living Lab is used as a test-bed, in which the BIPV/T system preheats ventilation air, while also, it is coupled with the building through an air-to-water heat pump and a thermal energy storage (TES) tank that serves as the heat source for the radiant floor heating (RFH). A detailed energy prediction model developed in TRNSYS is considered as a true representation of the building and it is used to identify the parameters of a low-order linear time-invariant state-space model. A simulation study using TMY3 data for West Lafayette, IN during the heating period shows that implementation of a deterministic MPC algorithm for the optimal set-point trajectory of the TES tank results in significant energy savings.

1. INTRODUCTION

Building-integrated photovoltaic-thermal (BIPV/T) systems can be attached to the building façade or replace conventional cladding (Figure 1), enabling on-site generation of solar electricity and heat. However, despite the substantial energy saving potential of this system, the utilization of the recovered heat from BIPV/T collectors is a complex issue. Also, given the variability of solar radiation, energy storage technologies are essential for the integration of BIPV/T systems in building operation.

Optimal control of buildings with integrated solar systems coupled with HVAC and energy storage is particularly complex, due to the variation of solar availability, the strong dependence on building load profile and the need to consider the interactions between design and control parameters. A control strategy that has shown significant potential for energy savings in buildings, wider user acceptance, and improved robustness with respect to building system variations and uncertainty compared with conventional approaches such as rule-based control or night setback is model predictive control (MPC). In this approach, a sequence of optimal control problems is solved with the most up-to-date information on system inputs and environmental disturbances and it is implemented in real-time.

Candanedo and Athienitis (2011) describe initial steps in this direction: with a BIPV/T-heat pump system as an additional heat source besides the ground source heat pump, in a solar house with a water thermal storage tank and radiant floor heating in Canada. The study developed a deterministic MPC formulation for selecting the set-point trajectory of the TES tank, using a transfer function model and an optimization algorithm based on dynamic programming. Quintana and Kummert (2014) developed optimal control strategies for solar district heating systems,

based on TRNSYS models and GenOpt as an optimizer. Pichler et al. (2014) developed a predictive controller for the auxiliary heating of a solar thermal combistorage system.

The present study, extends previous work on predictive control of buildings with integrated solar systems and thermal energy storage by: (a) considering its application to a high performance office building; (b) examining the potential impacts associated with the solar radiation prediction accuracy, since this is the most significant disturbance acting on the system; (c) investigating the impact of the optimal control trajectories for the TES on system energy costs. At the methodological level, this paper develops simplified models for the dynamic system under investigation, based on state-space representation (linear, time invariant), for the first time, using black-box system identification. In this study, the BIPV/T system is connected to an air-to-water heat pump, which serves as a heat source for the TES tank that is coupled with the building through the RFH system. These three components (BIPV/T, TES tank, RFH) are the integrated solar system within the context of this paper.
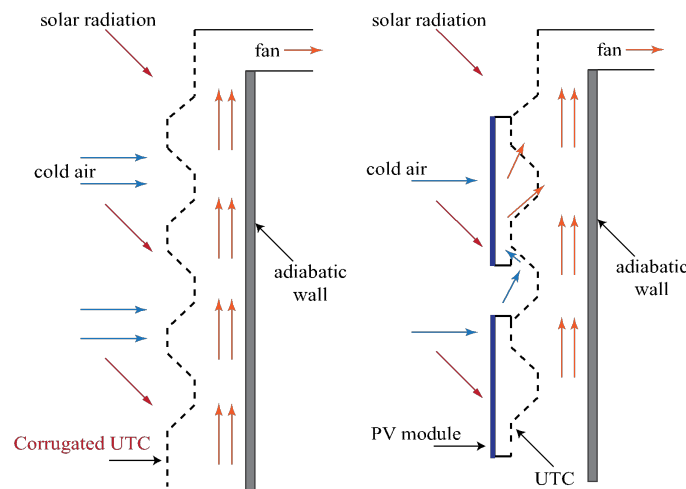

Figure 1 Sketch up of the corrugated transpired solar collector without (left) and with (right) PV panels

2. METHODOLOGY

2.1 Building Description

The Hydronic Lab (Figure 2), at the new Herrick Building at Purdue University, West Lafayette, IN, is considered as a test-bed in this study. It is one of the Living Labs, which are four office spaces located on the third floor of the building, with the Hydronic Lab located on the south-east corner. Table 1 provides information for the basic settings and HVAC systems used in the building and system model developed in TRNSYS.
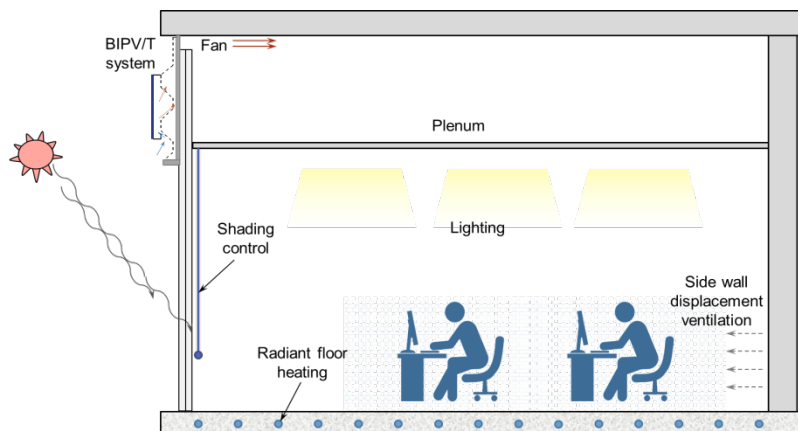

Figure 2 Section view of the test-building

Type 56 in TRNSYS is used for the building model, with standard ventilation and shading controls. The radiant floor heating is modeled using component type 653, with WFR of 600 kg/hr as the baseline case. A wide range of room temperature set-points is applied in the simulation, to account for the large thermal mass and slow dynamic response of the TES tank. Two prototype BIPV/T system configurations, i.e. a corrugated unglazed transpired solar collector (UTC), with and without PV panels, are investigated. These systems have been incorporated into TRNSYS as a user-defined component, using the energy models presented in Li et al. (2014) and Li and Karava (2014). In the present study, the BIPV/T system is assumed to be installed on the top section of the south façade (covering the plenum area), to avoid blocking daylighting (Figure 2). In this way, the BIPV/T system would be near the roof, facilitating placement of the ducts, heat pump and TES tank. The potential available area for the BIPV/T system is around 65 m^2. The PV panels have a nominal power of 0.108 kW/m^2 (Day4 Energy Inc., model: DAY418MC). For the UTC configuration with PV panels, the PV panel coverage ratio is around 90 %, based on optimal design recommendations presented in Li et al. (2014), which provide 58.5 m^2 available PV areas with 6.32 kWp (kilowatt-peak) capacities.

Table 1 Simulation settings

Room temperature	18 – 26 °C, 8:00 am – 10:00 am 21 – 26 °C, 10:00 am – 18:00 pm >15 °C, 18:00 pm – 8:00 am
Floor temperature	19 – 29 °C (ASHRAE Standard 55)
BIPV/T design	Total area: 65 m^2 PV area: 32 m^2, around 20 kWh/day Air flow rate: 5600 m^3/hr, corresponding suction velocity: 0.024 m/s
Shading control	ON, when the incident solar radiation on the window exceeds 180 W/m^2 OFF, when the incident solar radiation on the window drops below 160 W/m^2
Envelope properties	Exterior wall: U = 0.122 W/m^2.K, Gypsum board 0.016 m Interior wall: U = 0.207 W/ m^2.K, Gypsum board 0.032 m Window: U = 0.63 W/m.K, average solar transmittance = 0.228, average absorptance = 0.487, average SHGC = 0.327 Roof: U = 0.368 W/m^{2}K Floor: U = 0.689 W/m^{2}K, Concrete 0.165 m
Internal heat gain	Lighting: 10.76 W/m^2, for 8:00 am – 18:00 pm; 0 otherwise Equipment: 21.52 W/m^2, for 8:00 am – 18:00 pm; 0 otherwise Occupants: 75 W/person, for 8:00 am – 18:00 pm; 0 otherwise
Infiltration	Air change rate = 0.737/hr
Ventilation	0.06 cfm/ft^2 or 5 cfm/person, whichever is greater, supply air temperature: 22 °C

Figure 3 shows the interactions between the electric grid, the building, the integrated solar system and the HVAC system. The electricity generated by the BIPV/T system can be used in the building, or be sold back to the grid. Part of the collected heat is directed into the air handling unit for ventilation air preheat and the remaining amount is fed into an air-to-water heat pump to increase its efficiency. The heat pump is used to charge a TES tank, which is coupled with the building through the RFH. This system is subjected to several environmental disturbances, such as utility price, weather conditions and occupancy.

2.2 System Identification

The detailed model (e.g. high-order with non-linear dynamics) of the Hydronic Lab developed in TRNSYS is viewed as a true representation of the integrated system and it is used to identify the parameters of a simplified model that can be incorporated in real controllers. The simplified model adopted in this study is a linear, time-invariant, discrete-time, state space model. The objective of the system identification process is to find matrices A, B, C, D and K of the simplified model (Equation 1 and 2) subjected to unknown white noise e_k, based on given simulation results for the input vectors u_k and the output vector y_k. x_k is the state vector of the system. In the present study, the white noise e_k is assumed to be zero, since we are using simulation results and sufficient input parameters, rather than actual measurements, for the identification.

$$x_{k+1} = Ax_k + Bu_k + Ke_k \tag{1}$$
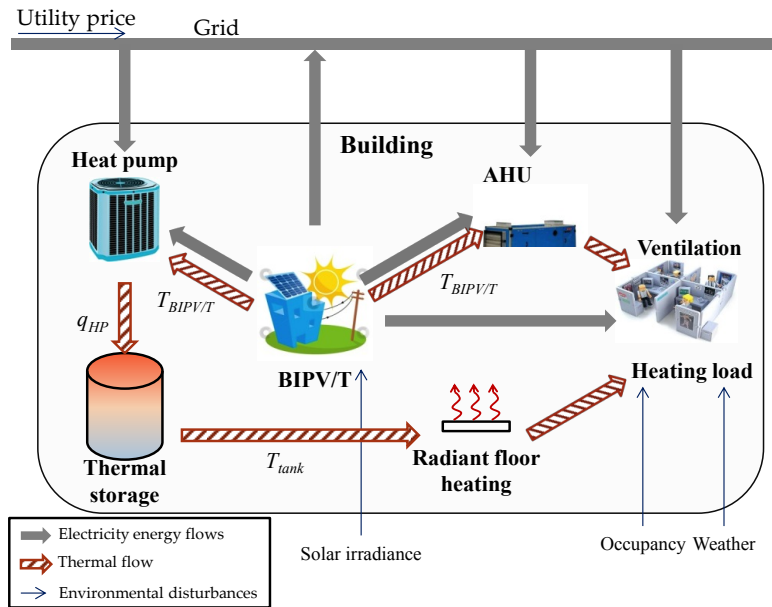
$$y_k = Cx_k + Du_k + e_k \tag{2}$$

Figure 3 The diagram of the integration between the electric grid, building, solar system and HVAC
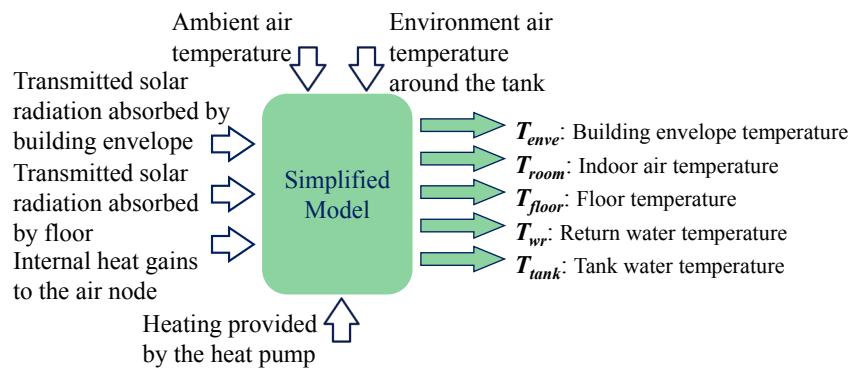

Figure 4 Inputs and outputs of the black-box model

Table 2 Identification results

Outputs	T_{enve}	T_{room}	T_{floor}	T_{wr}	T_{tank}
Training Data-Fit factor (%)	89.2	91.39	94.98	96.39	93.71
Training Data-RMSE (°C)	0.37	0.31	0.12	0.08	0.37
Calibration Data-RMSE (°C)	0.38	0.31	0.11	0.08	0.35

A subspace system identification (4SID) method is used to obtain a simplified model that can be used within the predictive controller. The 4SID method is a statistically based data-driven approach that is suitable for multiple-input-multiple-output systems (Overschee & Moor, 1999), and can handle large amount of data with minimum

computational resource requirements (e.g. it takes only 75 seconds to finish the identification for a 20th order model). This is a powerful approach for MPC implementation in real buildings, which are equipped with various sensors collecting input data and the controller needs to process large amounts of data in short time. Also, this approach does not require a detailed understanding of the building dynamics and complex physical phenomena in order to determine appropriate input and output variables. A detailed description of the method can be found in Overschee & Moor (1999) and Prívara et al. (2013). Among the different options, the N4SID algorithm is selected, for its availability in Matlab[®]. The inputs and outputs for the black-box model are shown in Figure 4. In this modeling representation, the states lose their physical meaning and an appropriate order needs to be determined to obtain the best fit with the training data. A common approach for the order selection suggests 2nd-3rd order dynamics per output temperature (Prívara et al. 2013), which leads to10[th] –15th order dynamics based on the five system outputs considered herein . Moreover, since the white noise of the system is set to be zero, a higher order n is required to reach better identification results. After testing the fitting error for 1-10th, 20th, 30th orders, a 20th order model turned out to have the best overall performance. Table 2 shows the identified parameter values along with the root mean square error (RMSE) for the training (2351 data points, from Jan 3rd to Feb 24th, 7 weeks) and calibration (336, from Feb 25th to Mar 3rd, 1 week) data sets, sampled every 30 minutes. Very good prediction accuracy can be observed with the maximum RMSE for the calibration data set equal to 0.38 °C and almost all the fit factors above 90 %.

2.3 Model Predictive Control Formulation

This section presents the deterministic MPC implementation for developing optimal trajectories of the TES tank set-point, formulated at a given point in time for a future planning horizon, based on the prediction of environmental disturbances (weather conditions, occupancy). The methodology is based on the assumption that future predictions are exact, with perfect knowledge of both the building system dynamics as well as all future disturbances acting upon the system. The control problem is formulated for analysis purposes, so it is a concept rather than an actual controller, to demonstrate the potential performance bounds for a given building using perfectly known historical data (TMY3). A prediction horizon of 48 hours is considered in this simulation study. A typical prediction horizon for this system would be 24 to 48 hours (Candanedo & Athienitis, 2011; Candanedo et al., 2013), depending on the capacity of the storage device. Although the objective of the study is to obtain the optimal T_{tank} trajectory, since this is an output of the simplified model, it cannot be controlled. Thus, the control variable in the MPC formulation is the heating power provided by the heat pump q_{hp}, or to be more precise, the heating power required to minimize the cost function while satisfying all the constraints. An electrical back-up heater is assumed to be placed inside the tank, in case the required heating power exceeds the maximum heating capacity of the heat pump. The efficiency of the heater is assumed to be 100 %. Figure 5 shows the flowchart for the deterministic MPC framework considered in the present study.

To develop the MPC framework, the following assumptions are made:
- The thermal stratification inside the TES tank is not taken into consideration, hence, the tank temperature is assumed to be uniform. The tank is assumed to be 1.25 m high. Based on simulation results using TRNSYS, the temperature difference between the top and bottom of the tank is negligible.
- For the air-to-water heat pump model, the inlet air temperature is assumed to be the same as the outlet air temperature from the BIPV/T system (T_{BIPVT}), although in reality, the inlet air temperature should be slightly lower due to losses. Similarly, the outlet water temperature of the heat pump is assumed to be the same as the tank temperature, for simplicity.
- For the cases considered, the optimal control sequence for the set-point trajectory of the TES tank is formulated over a 48-hr planning horizon, beginning at 6 am and it is repeated considering 2-hr intervals in order to maintain the decision space relatively small (it should be noted that the simulation time-step is 30 min in order to capture the important system dynamics). This implies that the heat input, q_{hp}, for each time step of the simplified model (30 minutes) is assumed to be the same within the 2 hours. With these 2-hr decision blocks, during which the operation of the heat pump is constant, the frequency of ON/OFF switching is reduced, improving the equipment overall performance. Furthermore, the heat pump is assumed to be OFF at night (10:00 pm – 6:00 am), in order to better utilize the solar energy availability during the day and reduce the operation cost (the Coefficient of Performance, COP, is usually lower at night, due to the low ambient temperature), while also reducing the decision space. There is only one exception to this assumption. When it is very cold, with the outdoor temperature lower than -15 °C, the heat pump operates at night as well to provide sufficient heat to the building.

- Besides the room and floor temperature settings presented in Table 1, the tank temperature is assumed to vary between 25 and 55 °C, based on the water outlet temperature operation range of the selected heat pump. This also eliminates the possibility to over-discharge the tank.
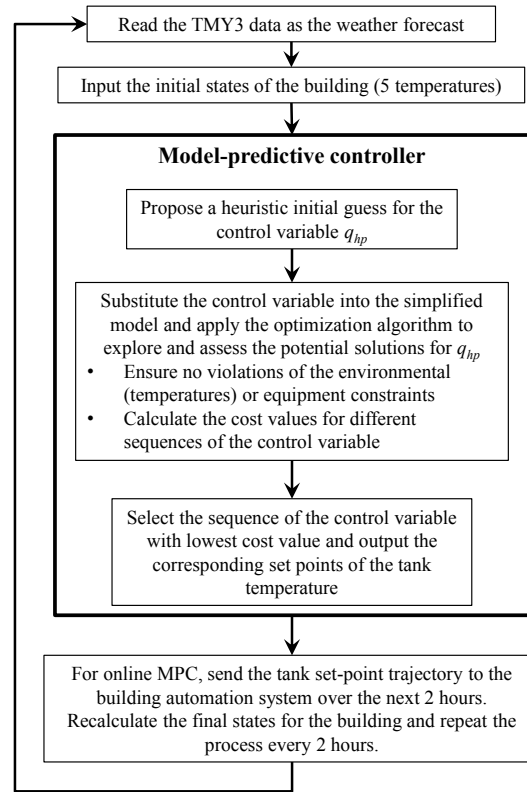

Figure 5 Flowchart of the MPC framework

An air-to-water heat pump is considered in the present study, instead of using an air-to-water heat exchanger and then a water-to-water heat pump, in order to reduce the heat loss during the heat transfer process. Verhelst et al. (2012) investigated four approaches to model the air-to-water heat pump performance with the following recommendations made: under the assumption that the heat pump operates on full load, the model with dependency on the supply water temperature and inlet air temperature results in the lowest energy cost with the same savings as the part load model, which also depends on the compressor frequency and accounts for the part load efficiency. Hence, the following heat pump model is adopted in the present study, due to its simplicity without sacrificing the performance, and the lack of part load data in the manufacturer's catalog:

$$COP = c_0 + c_1 T_{BIPVT} + c_2 T_{TANK} + c_3 T_{BIPVT}^2 + c_4 T_{TANK}^2 + c_5 T_{BIPVT} T_{TANK} \tag{3}$$

An important feature of the heat pump selected is its operation range for the inlet air temperature, T_{BIPVT}, in order to account for the benefits from the BIPV/T system. A heat pump from DAIKIN (model: ERLQ048BAVJU) is used with the coefficients for the COP (Equation 3) obtained based on data available in the manufacturer's catalog. The heat pump can operate for inlet air temperature varying between -20 to 20 °C, with COP between 2.3 (worst case scenario) and 6.58 (ideal scenario). The R^2-value of the regression results is equal to 0.988 and the average and maximum deviation are equal to 1 % and 5 %, respectively.

The objective function J_{tot} in the MPC formulation is the accumulated electrical energy consumption (J_e) over the prediction horizon (N) subjected to thermal comfort and equipment constraints as follows:

$$\min_t J_{tot} = \sum_{t=0}^{N} J_e(t)$$

$$\tag{4}$$

Subject to: $P_{hp} \in [0, HC/COP]$;

$T_{TANK} \in [25,55]°C$;

$T_{floor} \in [19,29]°C$;

$T_{room} \in [T_{room_{min}}, T_{room_{max}}]°C$, based on the values and schedules given in Table 1.

For each time step (30 minutes), the electrical energy consumption of the heat pump P_{hp} is calculated as q_{hp}/COP, in which the calculation of COP is affected by the solar radiation, ambient air temperature and the tank temperature as described in Equation 3.

When the required heating power exceeds the maximum heating capacity of the heat pump (*HC*), calculated using Equation 5, the backup heater provides the extra heating power to meet the thermal comfort constraints. The coefficients in Equation 5 are obtained through the same quadratic fit of the catalogue data as Equation 3, with the same R^2-value and deviation percentages.

$$HC = b_0 + b_1 T_{BIPVT} + b_2 T_{TANK} + b_3 T^2_{BIPVT} + b_4 T^2_{TANK} + b_5 T_{BIPVT} T_{TANK} \qquad (5)$$

The electrical energy consumption can then be calculated with Equation 6, in which, c_{el} is the utility electricity price that may vary with time. The electricity price is assumed to be constant in this paper. P_{heater} is the electricity consumption of the back-up heater, kWh.

$$J_e = c_{el}(t)[P_{hp}(t) + P_{heater}(t)] \qquad (6)$$

The pattern search algorithm available in Matlab® toolbox is used for the solution of the non-linear, constrained optimization problem. Pattern search is essentially a grid search on the control variable, where an initial guess is made and points in a grid around that guess are evaluated for a more optimal solution. The algorithm continues to search the grid until no more optimal solutions can be found, at which point it reduces the size of the grid and searches locally around the current most optimal solution identified by the larger grid. Detailed information about pattern search can be found in Matlab's Global Optimization Toolbox or in Torczon (1997) and Lewis et al., (2000). The algorithm has been previously used in optimal control studies for buildings.

3. RESULTS AND DISCUSSION

This section presents the simulation study performed using TMY3 data for West Lafayette, IN to test the performance of the predictive controller (offline MPC) during the heating period. The initial short-term evaluation considers the following two scenarios: a sunny day and a cloudy day, respectively, after two consecutive sunny days. Since the TES tank is used to store solar energy during the daytime for use during the night or the next day, these two simulation scenarios are set up to study the impact of how the next day weather affects the decisions made by the optimal controller. The tank volume considered in this section is 5 m^3 so that it can approximately store thermal energy to satisfy the average daily heating load requirements of the building, calculated based on simulations over the entire heating season (October to March).

3.1 Scenario one: three consecutive sunny days

Simulations are performed for a period of four days and Figure 6ashows the simulation results for scenario one, i.e. three consecutive days (Feb 2rd to Feb 4th) with outdoor temperature variation between -14 to 2 °C. Simulation results for the fourth day are not shown, as the tank is designed to satisfy the heating requirements for an extra day and hence, there is no need to operate the heat pump on the fourth day. During sunny days, the heat pump operates to fulfill the heating requirement of the building, and also charge the TES tank during the day time, utilizing the solar energy collected through the BIPV/T system. The set point of the tank temperature is influenced by many factors, for instance, it should be high enough to meet the thermal comfort requirements of the building, but below a certain value to avoid overheating. The MPC strategy can ensure that the heat pump only charges the tank when there are benefits to do so. As shown in Figure 6a, the heat pump operation follows the solar energy availability. The heating power boosts in the morning are due to the temperature settings. The comparison between the heating power and the actual electrical power indicates a significant efficiency increase due to the solar radiation. For example, the

heating power between 829 to 839 hours is constant (even lower towards the hour 839), while the electrical consumption increases from 2 kW to 3.2 kW, along with the reduction of the solar irradiance.

The heating power provided on the third day is much lower than the two previous days, due to the following reasons: firstly, the outdoor temperature is about 2 °C higher than the previous two days, which leads to lower heating load; secondly, the solar radiation on the first two days is strong and the tank has stored sufficient energy for the third day; thirdly, the solar radiation on the third day reaches a high peak, but the total amount is less than the previous two days, so there is less energy to be stored. The total electrical energy consumption for the three days is 84 kWh with energy stored to satisfy the needs for one more day, while the corresponding heating load for the total four days is 690.3 kWh. This gives an equivalent COP of 8.22.

3.2 Scenario two: one cloudy day after two consecutive sunny days

Figure 6b shows the simulation results for scenario two, i.e. three consecutive days (Feb 9th – Feb 11th) with outdoor temperature variation between -15 to 1 °C, and corresponding heating load of 491.3 kWh (Feb 9th – Feb 12th). The solar radiation on the third day is very low (close to zero) and the total incident solar radiation on the south façade during the three days is 1.8 kWh/m^2 less than in scenario one. As a result, the outlet air temperature of the BIPV/T system cannot be raised to a desired value to increase the heat pump COP. The tank temperature is generally higher, compared to the previous case, and the heat pump provides an almost constant heating power on the third day, since there is no significant variation on the COP due to the BIPV/T. During the three days, the heat pump consumes 116 kWh of electrical power in total, which is 38 % higher compared to scenario one, despite the lower total heating load requirement. The equivalent system COP is 4.24.

3.3 Monthly analysis

Simulation was performed for a period of one month during the heating season to compare the total and detailed energy cost for the following systems:
1) S1: the baseline RFH;
2) S2: RFH with the TES tank, heat pump and MPC strategy but no solar systems;
3) S3: the integrated solar system with the MPC formulation and the configuration of UTC only (studied in previous Sections);
4) S4: the integrated solar system with the MPC formulation and the configuration of UTCs integrated with PV panels (Figure 1, right).
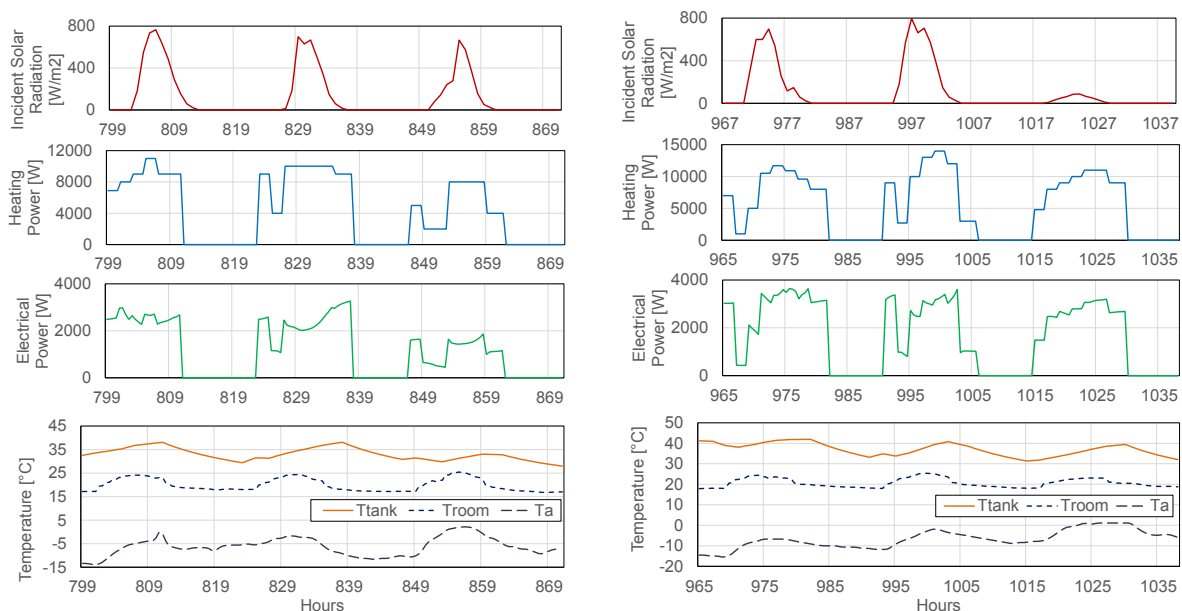

Figure 6 Simulation results for (a) scenario one (left) and (b) scenario two (right)

February (plus the first three days of March, 31 days total) was selected for its low outdoor temperature and significant heating requirement, as well as the solar availability. The zone heating load of this month is 3900 kWh, excluding the ventilation energy needs. Simulation results are shown on Figure 7 and are presented in terms of ventilation thermal energy, heat pump electrical energy, PV energy output and the total energy cost. The heat pump electrical energy cost for system S1 is calculated by dividing the building heating load by an average COP , which is assumed to be 3.5. It can be seen that when there is no solar system (S1 and S2), the PV electrical output and fan electrical energy cost are zero and the ventilation energy cost is the same for both systems. However, with integrated RFH and TES tank and MPC implementation, the heat pump electrical energy saving is about 10.8 %, even without the solar system to increase the heat pump efficiency. When comparing systems S2 and S3, integration of the solar system (S3) can provide energy savings of 9.5 % and 13.5 % on the ventilation and heat pump energy cost, respectively. This gives 17.4 % total energy saving compared to system S1 and 11.7 % saving comparing to system S2.

The system S4 is integrated with PV panels, which offers electricity generation with a reduction in thermal energy collection, as the ventilation and heat pump energy cost are both higher in S4 than in S3, and the energy saving potential introduced by the solar thermal energy, reduces to 6.7 % compared to S2. However, when considering the electricity generation, the energy saving potential is the highest among the four systems, which is 33.9 %, 41.6 % and 45.4 %, respectively, comparing to S3, S2 and S1.
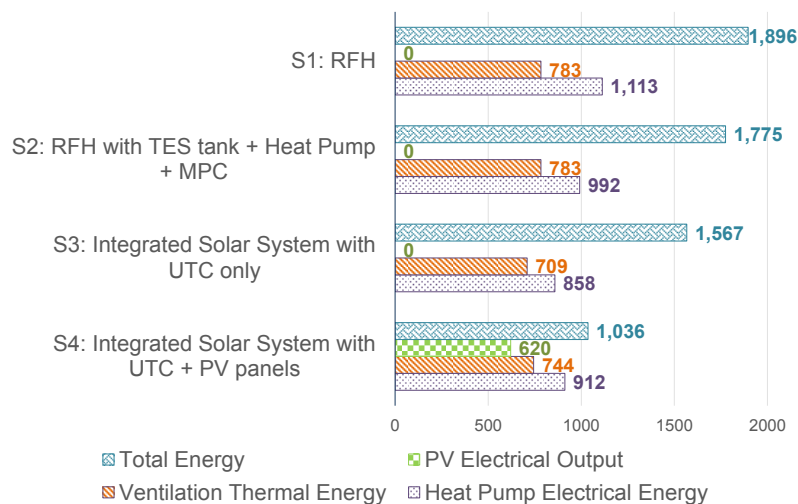

Figure 7 Detailed energy cost for different system integrations approaches and control strategies

4. Conclusions

The paper demonstrates a methodology for developing a deterministic MPC strategy for an integrated solar system. This includes building up a detailed dynamic system model in TRNSYS, presenting a system identification approach to obtain a simplified model that can be implemented within the predictive controller, formulating the cost function and setting up the constraints and the optimization environment. A simulation study is also performed to analyze the parameters that have profound impacts on the MPC performance and to quantify the energy saving potential of the controller and the integrated solar system in comparison to a baseline RFH system. The test-building has a hydronic floor and a thermal energy storage device, with slow response to environment excitations. This type of system requires a large amount of energy to change its current state and thus, efficient integration concepts and optimal control strategies are necessary to predict and plan the energy cost. Based on the outcomes of this study, predictive control strategies implemented in the solar system and can achieve significant energy savings.

Finally, the simulation results for different systems show that only adding the TES tank and MPC strategy to the regular RFH system can result in 10.8 % energy saving of the heat pump electrical energy cost. When integrating the UTC plates to the system (S3), the total energy saving is 17.4 % comparing to regular RFH system. Utilizing the

configuration of UTCs with PV panels can result in 45.4 % total energy saving compared to the baseline RFH due to the electricity generation by the PV panels. This energy saving potential is applicable to the RFH system considered in this paper. In practice, selecting the BIPV/T system configuration depends on the specific application and design intent.

REFERENCES

Candanedo, J.A. and Athienitis A.K., 2011. Predictive control of radiant floor heating and solar-source heat hump operation in a solar house. *HVAC&R Research* 17(3): 235–56.

Candanedo, J.A., Dehkordi, V.R. and Stylianou, M., 2013. Model-based predictive control of an ice storage device in a building cooling system. *Applied Energy* 111: 1032-1045.

Hu, J. and Karava, P. 2014. Model predictive control strategies for buildings with mixed-mode cooling. *Building and Environment* 71: 233-244.

Lewis, R.M., and Torczon, V., 2000. Pattern Search Methods for Linearly Constrained Minimization. *SIAM Journal on Optimization* 10(3): 917–941.

Li, S., Karava, P., Currie, S., Savory, E. and Lin, W.E. 2014. Energy modeling of photovoltaic thermal systems with corrugated unglazed transpired solar collectors–Part 1: Model development and validation. *Solar Energy* 102: 282–296.

Li, S. and Karava, P. 2014. Energy modeling of photovoltaic thermal systems with corrugated unglazed transpired solar collectors–Part 2: Model development and validation. *Solar Energy* 102: 297–307.

Overschee, P.V. and Moor, B.D., 1999. *Subspace Identification for Linear Systems*, Kluwer Academic Publishers, Nowell, MA.

Pichler, M. F., Lerch, W., Heinz, A., Goertler G., Schranzhofer H., Rieberer R., 2014. A novel linear predictive control approach for auxiliary energy supply to a solar thermal combistorage. *Solar Energy*. 101, 203–219.

Prívara, S., Cigler, J., Váňa, Z., Oldewurtel, F., Sagerschnig, C. and Žáčeková, E., 2013. Building modeling as a crucial part for building predictive control. *Energy and Buildings* 56: 8-22.

Quintana, H. J. and Kummert M., 2014. Optimized control strategies for solar district heating systems. *Journal of Building Performance Simulation*. DOI: 10.1080/19401493.2013.876448

Torczon, V., 1997. On the Convergence of Pattern Search Algorithms. *SIAM Journal on Optimization* 7(1): 1–25.

Verhelst, C., Logist, F., Van Impe, J. and Helsen, L., 2012. Study of the optimal control problem formulation for modulating air-to-water heat pumps connected to a residential floor heating system. *Energy and Buildings* 45: 43-53.